

## Discovery of Potent Competitive Inhibitors of Indoleamine 2,3-Dioxygenase with in Vivo Pharmacodynamic Activity and Efficacy in a Mouse Melanoma Model

Eddy W. Yue, Brent Douty, Brian Wayland, Michael Bower, Xiangdong Liu, Lynn Leffet, Qian Wang, Kevin J. Bowman, Michael J. Hansbury, Changnian Liu, Min Wei, Yanlong Li, Richard Wynn, Timothy C. Burn, Holly K. Koblish, Jordan S. Fridman, Brian Metcalf, Peggy A. Scherle, and Andrew P. Combs\*

*Incyte Corporation, Experimental Station, Route 141 and  
Henry Clay Road, Wilmington, Delaware 19880*

Received April 23, 2009

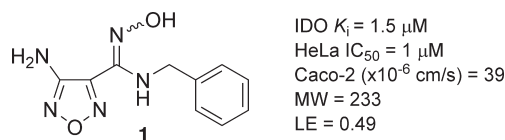
**Abstract:** A hydroxyamidine chemotype has been discovered as a key pharmacophore in novel inhibitors of indoleamine 2,3-dioxygenase (IDO). Optimization led to the identification of **1**, which is a potent (HeLa  $IC_{50}$  = 19 nM) competitive inhibitor of IDO. Testing of **1** in mice demonstrated pharmacodynamic inhibition of IDO, as measured by decreased kynurenine levels (> 50%) in plasma and dose dependent efficacy in mice bearing GM-CSF-secreting B16 melanoma tumors.

Indoleamine 2,3-dioxygenase (IDO<sup>a</sup>) and tryptophan 2,3-dioxygenase (TDO) are the two key heme-containing dioxygenases that catalyze the rate limiting step in the catabolism of the essential amino acid tryptophan to *N*-formylkynurenine by oxidative cleavage of the indole 2,3 double bond.<sup>1</sup> This reaction is the initial step in the de novo biosynthetic route, known as the kynurenine pathway, which leads to a series of biologically active metabolites, including neurotransmitters serotonin and melatonin, excitotoxin quinolinic acid, *N*-methyl-D-aspartate (NMDA) receptor antagonist kynurenic acid, and ultimately the production of nicotinamide adenine dinucleotide (NAD). IDO is expressed in various tissues throughout the body but predominately in cells within the immune system where it is specifically induced in dendritic cells and macrophages at sites of inflammation by cytokines, such as interferon  $\gamma$  (IFN- $\gamma$ ).<sup>1</sup> The overexpression of IDO has been implicated in a variety of diseases, including cancer, neurodegenerative disorders (Alzheimer's disease), age-related cataract, and HIV encephalitis.<sup>2–6</sup> In contrast, TDO is almost entirely located in the liver where it maintains proper tryptophan balance in response to dietary intake.

Recently, IDO has been shown to play an important role in the process of immune evasion by tumors.<sup>1</sup> IDO mediated depletion of local tryptophan levels, and production of toxic tryptophan metabolites results in suppression of T cell activation and induction of T cell apoptosis. The overexpression of

IDO in tumor cells, as well as in the dendritic cells that localize to the tumor draining lymph nodes, has been shown to be an independent prognostic variable for reduced overall survival in patients with in a wide variety of tumors, including ovarian, colorectal, and pancreatic cancers, melanoma, and hematological malignancies.<sup>7</sup> Further, it was shown that 1-methyltryptophan (1-MT), a weak competitive inhibitor ( $K_i$  = 34  $\mu$ M) of the enzyme, increases the efficacy without increased toxicity of chemotherapeutic agents, such as paclitaxel, gemcitabine, and cyclophosphamide, in several mouse tumor models.<sup>9</sup> As a single agent, 1-MT impairs the growth of granulocyte-macrophage colony-stimulating factor (GM-CSF) expressing B16 melanomas.<sup>8</sup> These effects were not observed in T cell deficient mice, suggesting that the results were a consequence of pharmacological inhibition of IDO mediated immunosuppression within the tumor microenvironment.

To date, only a few structural classes are known to be IDO inhibitors. Most of these compounds have been shown to be noncompetitive inhibitors and likely are involved in redox reactions with the iron bound to the heme of IDO.<sup>8–12</sup> Nearly all of the reported competitive IDO inhibitors are structurally related tryptophan analogues, such as 1-MT.<sup>13–16</sup> The modest potencies and poor physical properties of these indole-based compounds led us to search for a new chemotype. A screening effort was initiated with the objective of identifying a novel lead compound that could be optimized to afford potent and selective inhibitors of IDO with suitable permeability and metabolic stability to allow evaluation of the functional consequences of IDO inhibition in vivo. Herein, we report the discovery and optimization of a novel structural series of potent and competitive inhibitors of IDO that strongly support the role of IDO in tumor progression and its pharmacological inhibition as a means to treat IDO overexpressing malignancies.

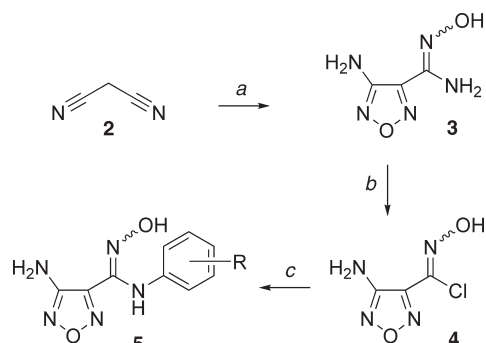


**Figure 1.** IDO lead **1**.

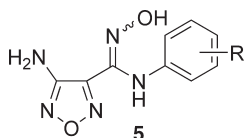
High throughput screening (HTS) of Incyte's corporate collection identified 4-amino-1,2,5-oxadiazole-3-carboximide (**1**) as a micromolar IDO enzyme inhibitor (Figure 1). Enzyme kinetic assays measuring the conversion of tryptophan to *N*-formylkynurenine demonstrated that **1** is a competitive inhibitor ( $K_i$  = 1  $\mu$ M). Direct binding to the heme active site was confirmed by absorption spectroscopy of the ferrous ( $Fe^{2+}$ ) form of IDO. Changes in the strength and maximum wavelength for the Soret peak suggest direct binding to the heme moiety. Testing in a human HeLa cell line stimulated with IFN- $\gamma$  to overexpress IDO provided further evidence that **1** is a potent inhibitor ( $IC_{50}$  = 1  $\mu$ M) of IDO. Counterscreening against TDO ( $IC_{50}$  = 10  $\mu$ M) demonstrated this class of inhibitor was selective for IDO. The combination of low molecular weight (<250), good ligand efficiency (LE = 0.49), low micromolar cellular activity, TDO selectivity, and high caco-2 permeability ( $39 \times 10^{-6}$  cm/s) of lead **1** provided an excellent starting point for our discovery program.

\*To whom correspondences should be address. Phone: 302-498-6832. Fax: 302-425-2750. E-mail acombs@incyte.com.

<sup>a</sup> Abbreviations: IDO, indoleamine 2,3-dioxygenase; TDO, tryptophan 2,3-dioxygenase; NAD, nicotinamide adenine dinucleotide; IFN- $\gamma$ , interferon  $\gamma$ ; 1-MT, 1-methyltryptophan; NMDA, *N*-methyl-D-aspartate; GM-CSF, granulocyte-macrophage colony-stimulating factor; Kyn, kynurenine; HTS, high throughput screening; SAR, structure–activity relationships; LE, ligand efficiency; TGC, tumor growth control.

**Scheme 1.** Synthesis of 4-Amino-1,2,5-oxadiazole-3-carboximidamides (**5**)<sup>a</sup>

<sup>a</sup> Reagents: (a) NaNO<sub>2</sub>, 2 N HCl, NH<sub>2</sub>OH·HCl; then 10 N NaOH, Δ, 2 h (see ref 18); (b) NaNO<sub>2</sub>, HCl, H<sub>2</sub>O, 0 °C, 1.5 h, 30–40% (see ref 19); (c) aniline, Et<sub>3</sub>N, EtOH, 0–25 °C, 30–60%.

**Table 1.** SAR of Phenyl Ring of 4-Amino-1,2,5-oxadiazole-3-carboximidamides (**5**)

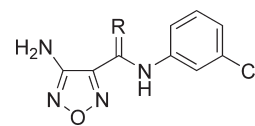
compd	R	IC <sub>50</sub> (nM) <sup>a</sup>	
		IDO	HeLa
<b>5a</b>	H	3200	490
<b>5b</b>	2-Cl	6500	1500
<b>5c</b>	3-Cl	86	19
<b>5d</b>	4-Cl	6000	2400
<b>5e</b>	3-F	500	270
<b>5f</b>	3-Br	73	17
<b>5g</b>	3-Me	550	120
<b>5h</b>	3-Et	430	54
<b>5i</b>	3-isopropyl	2100	225
<b>5j</b>	3- <i>tert</i> -butyl	25000	6800
<b>5k</b>	3-OMe	4400	970
<b>5l</b>	3-Cl,4-F	67	19 (46) <sup>b</sup>
<b>5m</b>	3-Br,4-F	59	12

<sup>a</sup> IC<sub>50</sub> values are the mean of at least three independent assays.

<sup>b</sup> Murine cellular B16 assay IC<sub>50</sub> (nM).

4-Amino-1,2,5-oxadiazole-3-carboximidamides **5** were synthesized in three steps (Scheme 1). Treatment of malononitrile **2** with hydroxylamine, sodium nitrite, and hydrochloric acid gave hydroxyamidine **3**,<sup>17</sup> which was diazotized under acidic conditions<sup>18</sup> to provide the hydroximoyl chloride **4**.<sup>19</sup> Coupling of **4** to a variety of benzylamines and anilines gave moderate yields of analogues **1** and **5**, respectively.

A diverse library of carboximidamides were synthesized and tested for their ability to inhibit human IDO in the standard enzymatic assay and a HeLa cellular assay measuring kynurenine formation spectrophotometrically (Table 1). We did observe that most compounds are slightly more potent in the more physiologically relevant HeLa cell-based assays than in the enzyme assays. This may be due to the complexity of the enzyme assay which utilizes a methylene blue ascorbate regeneration system to maintain IDO in the active reduced form or unidentified differences between the recombinant IDO used in the enzyme assay and native IDO in HeLa cells. Nevertheless, a very good correlation between the two assays

**Table 2.** SAR of the Hydroxyamidine

compd	R	IC <sub>50</sub> (nM) <sup>a</sup>	
		IDO	HeLa
<b>5c</b>	N-OH	90	20
<b>6</b>	N-OMe	> 20000	> 2000
<b>7</b>	NH	> 20000	> 2000
<b>8</b>	N-NH <sub>2</sub>	1400	> 2000
<b>9</b>	O	> 20000	> 2000
<b>10</b>	S	> 20000	> 2000

<sup>a</sup> IC<sub>50</sub> values are the mean of at least two independent assays.

is observed and enabled optimization by iterative cycles of synthesis and testing.

Early structure–activity relationships (SAR) demonstrated that phenyl derivatives **5** were significantly more potent than the original benzyl lead **1** and other alkylamine derivatives. Selected phenyl analogues and their SAR are shown in Table 1. A strong preference for meta-substitution was demonstrated by the 50-fold improvement in cellular potency when *m*-chloro **5c** was compared to *o*-chloro **5b** and *p*-chloro **5d**. A variety of other ortho- and para-substituents larger than fluoro were also significantly less active (data not shown). Further optimization revealed that meta-halogens and small meta-alkyl substituents provided the most potent IDO inhibitors in this series (Br, Cl > Me, Et > isopropyl, *F* > H, OMe *tert*-butyl), including *m*-chloro **5c** and *m*-bromo **5g** (HeLa IC<sub>50</sub> = 19 and 17 nM, respectively). Addition of a *p*-fluoro substituent to these derivatives was tolerated and gave **5l** and **5m**, which showed improved in vitro human intrinsic clearances (**5c** = 1.1, **5l** = 0.57 L/h/kg) without loss in IDO cellular potency. **5l** was chosen for further in vitro and in vivo studies because of its improved physical chemical properties compared to **5m**. Counterscreening against TDO showed **5l** was inactive (IC<sub>50</sub> > 10 μM) in our TDO enzyme and cellular assays. Membrane permeability remained excellent for all compounds in the series, for example, **5l** caco-2 permeability = 36 × 10<sup>-6</sup> cm/s. We speculate the reason compounds within this chemotype have high permeability is due to a combination of their low molecular weight and low energy conformation containing two internal hydrogen bonds.

SAR of the unique hydroxyamidine functional group demonstrated its important role in binding IDO. All modifications of the hydroxyamidine pharmacophore gave significantly less potent derivatives (Table 2). Amide **9** and thioamide **10** were devoid of activity. Elimination of only the hydroxyl group in amidine **7** or methylation of the hydroxyl group in methoxyamidine **6** revealed the requirement for a free hydroxyl group to bind IDO. Only the aminoamidine **8** showed measurable activity, albeit 300-fold less active in the HeLa cell assay. In accordance with the SAR established here, the known binding of compounds containing hydroxyamidines to iron hemes, and our internal enzyme kinetics and spectroscopic results, we hypothesize that these IDO inhibitors form a dative bond with the heme iron in the ferrous state through the oxygen of the hydroxyamidine.

A computer model of **5l** bound to IDO was generated on the basis of the published crystal structure of IDO and established

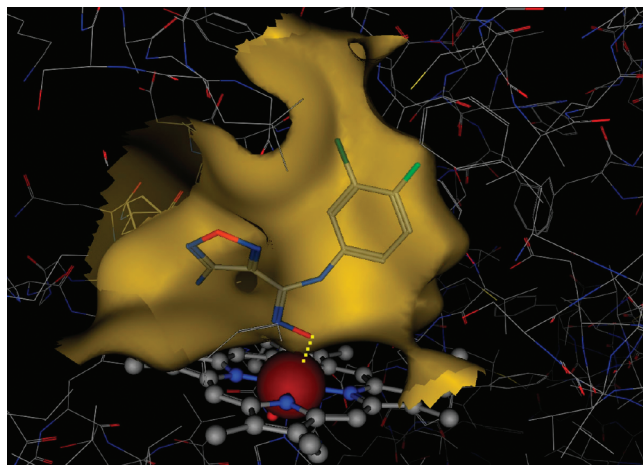


**Figure 2.** Computer generated model of **5I** bound to hIDO using the Molecular Operating Environment (MOE) from Chemical Computing Group. The coordination of the oxygen of the hydroxyamidine to the iron (red ball) of the heme (ball and stick) is shown as a dotted yellow line.

SAR for the series (Figure 2).<sup>20,21</sup> The initial modeling of **5I** to IDO assumed that the oxygen of the hydroxyamidine coordinates with the heme iron in the catalytically active, ferrous ( $\text{Fe}^{2+}$ ) state. Conformational analysis of **5I** in solution revealed that the compound exists in a low energy cis-conformation which is consistent with published crystal structures of similar hydroxyamidines that also form an intramolecular hydrogen bond between the aniline nitrogen and the oxygen of the hydroxyamidine.<sup>22</sup>

The phenyl ring was then placed deep into the hydrophobic pocket where it is perfectly situated to extend a meta-substituent into a small hydrophobic channel. In this conformation, the phenyl ring fits tightly into the active site, providing strong rationale for the lack of activity of compounds bearing substituents larger than hydrogen or fluoro in the ortho- and para-positions. The furazan moiety extends toward solvent, making loose contacts with the enzyme. The amino substituent is situated in the vicinity of a propanoic acid group on the heme ring where it may form a hydrogen bond.

IDO inhibitor **5I** was selected for further evaluation in vivo. The reduction of kynurenine levels in plasma was used as a pharmacodynamic marker for inhibition of IDO activity. Initial oral pharmacokinetic studies showed that **5I** was rapidly cleared ( $t_{1/2} < 0.5$  h) and that oral administration would not be a suitable dosing method for in vivo studies. Therefore, a single subcutaneous 100 mg/kg dose of **5I** was administered to naive C57BL/6 mice. Blood was harvested from individual mice over 8 h. Kynurenine and inhibitor **5I** concentrations were measured by LCMS. Reductions of kynurenine levels by ~50–60% were observed between 2 and 4 h, with maximum inhibition seen at 2.5 h (Table 3). The measured plasma exposure (2.5  $\mu\text{M}$ ) of **5I** during this period exceeded our calculated mouse protein binding adjusted B16 cellular  $\text{IC}_{50}$  ( $\text{PB}_{\text{adj}}\text{IC}_{50} = 1.0 \mu\text{M}$ , murine cellular B16  $\text{IC}_{50} = 46$  nM). Notably, kynurenine levels increased back to baseline after 4 h as **5I** exposure levels decreased below the mouse  $\text{PB}_{\text{adj}}\text{IC}_{50}$  from 1.0 to 0.1  $\mu\text{M}$ .

The efficacy of **5I** was tested in C57BL/6 mice bearing GM-CSF-secreting B16 tumors, where 1-MT has previously shown activity.<sup>23</sup> Tumors were allowed to grow until day 7 when 14 days of subcutaneous dosing of **5I** at 25, 50, and 75 mg/kg b.i.d. was initiated. Dose dependent inhibition of tumor

**Table 3.** **5I** Suppresses Kynurenine Generation in Vivo<sup>a</sup>

group	plasma Kyn ( $\mu\text{M}$ )	Kyn (% inh)	<b>5I</b> ( $\mu\text{M}$ )
control	1.1 $\pm$ 0.17		
2.5 h	0.45 $\pm$ 0.2	60	2.5 $\pm$ 0.6

<sup>a</sup>Data are averaged from three individual mice per treatment per time point.

**Table 4.** **5I** Inhibits B16-GMCSF Melanoma Growth in C57BL/6 Mice<sup>a</sup>

<b>5I</b> dose (mg/kg b.i.d.)	TGC (day 20) (%)	<b>5I</b> at 1 h ( $\mu\text{M}$ )
25	13	8.9 $\pm$ 1.2
50	36 <sup>b</sup>	12 $\pm$ 1.2
75	50 <sup>c</sup>	29 $\pm$ 13

<sup>a</sup>Data provided are from one of two experiments with similar results. <sup>b</sup> $p < 0.05$  vs vehicle control. <sup>c</sup> $p < 0.01$  vs vehicle control.

growth was correlated with increasing exposures of **5I** in plasma (Table 4).

These levels exceed those necessary to reduce kynurenine in plasma by > 50%. A maximal effect of 50% tumor growth control (TGC) was seen when **5I** was administered subcutaneously at 75 mg/kg b.i.d. ( $p < 0.01$ ). For comparison, 1-MT demonstrated ~45% TGC when administered as subcutaneous pellets (5 mg/day).<sup>23</sup> Taken together, these data suggest that this novel hydroxyamidine structural class, represented by **5I**, can inhibit IDO in vivo, as measured by pharmacodynamic reduction in kynurenine levels and tumor growth suppression.

A competitive hydroxyamidine containing IDO inhibitor **1** was identified by high throughput screening. Modification of the scaffold afforded a novel and potent IDO inhibitor **5I** with > 100-fold improvement in enzyme and cellular potency. A computer model of **5I** bound to IDO through the oxygen of the hydroxyamidine to the iron of the heme in the ferrous state was consistent with enzyme kinetics and SAR for the series. Testing in mice demonstrated that **5I** decreased kynurenine levels by > 50% in plasma and inhibited B16-GM-CSF tumor growth in a dose dependent fashion. These data provide convincing support for pharmacological inhibition of IDO as a means to disable tumor-induced immune tolerance and to treat a variety of cancers where IDO is overexpressed.

**Acknowledgment.** We thank Laurine Galya, Mei Li, James Doughty, and Karl Blom for their analytical assistance. We thank Mary Becker-Pasha and Mark Rupar for production of the enzyme and development of the IDO and TDO enzyme assays, respectively. We also thank Dr. Hyam Levitsky at Johns Hopkins University School of Medicine for providing us with the B16-GM-CSF cell line.

**Supporting Information Available:** Synthesis procedures with supporting analytical data and assay protocols. This material is available free of charge via the Internet at <http://pubs.acs.org>.

## References

- (1) Munn, D. H.; Mellor, A. L. Indoleamine 2,3-dioxygenase and tumor-induced tolerance. *J. Clin. Invest.* **2007**, *117*, 1147–1154.
- (2) Takikawa, O. Biochemical and medical aspects of the indoleamine 2,3-dioxygenase-initiated L-tryptophan metabolism. *Biochem. Biophys. Res. Commun.* **2005**, *338*, 12–19.
- (3) Boasso, A.; Herbeuval, J.-P.; Hardy, A. W.; Anderson, S. A.; Dolan, M. J.; Fuchs, D.; Shearer, G. M. HIV inhibits CD4+ T-cell proliferation by inducing indoleamine 2,3-dioxygenase in plasmacytoid dendritic cells. *Blood* **2007**, *109*, 3351–3359.

- (4) Potula, R.; Poluektova, L.; Knipe, B.; Chrastil, J.; Heilman, D. Dou, H.; Takikawa, O.; Munn, D. H.; Gendelman, H. E.; Persidsky, Y. Inhibition of indoleamine 2,3-dioxygenase (IDO) enhances elimination of virus-infected macrophages in an animal model of HIV-1 encephalitis. *Blood* **2005**, *106*, 2382–2390.
- (5) Guillemain, G. J.; Brew, B. J.; Noonan, C. E.; Takikawa, O.; Cullen, K. M. Indoleamine 2,3 dioxygenase and quinolinic acid immunoreactivity in Alzheimer's disease hippocampus. *Neuropath. Appl. Neurobiol.* **2005**, *31*, 395–404.
- (6) Fujigaki, H.; Saito, K. Inhibition of increased indoleamine 2,3-dioxygenase activity exacerbates neuronal cell death in various CNS disorders. *Int. Congr. Ser.* **2007**, *1304*, 314–323.
- (7) Curti, A.; TrabANELLI, S.; Salvestrini, V.; Bacarani, M.; Lemoli, R. M. The role of indoleamine 2,3-dioxygenase in the induction of immune tolerance: focus on hematology. *Blood* **2009**, *113*, 2394–2401.
- (8) Peterson, A. C.; La Loggia, A. J.; Hamaker, L. K.; Arend, R. A.; Fisette, P. L.; Ozaki, Y.; Will, J. A.; Brown, R. R.; Cook, J. M. Evaluation of substituted beta-carbolines as noncompetitive indoleamine 2,3-dioxygenase inhibitors. *Med. Chem. Res.* **1993**, *473*–482.
- (9) Carr, G.; Chung, M. K. W.; Mauk, A. G.; Andersen, R. J. Synthesis of indoleamine 2,3-dioxygenase inhibitory analogues of the sponge alkaloid exiguamine A. *J. Med. Chem.* **2008**, *51*, 2634–2637.
- (10) Pereira, A.; Vottero, E.; Roberge, M.; Mauk, A. G.; Andersen, R. J. Indoleamine 2,3-dioxygenase inhibitors from the Northeastern Pacific marine hydroid *Garveia annulata*. *J. Nat. Prod.* **2006**, *69*, 1496–1499.
- (11) Brastianos, H. C.; Vottero, E.; Patrick, B. O.; Van Soest, R.; Matainaho, T.; Mauk, A. G.; Andersen, R. J. Exiguamine A, an indoleamine-2,3-dioxygenase (IDO) Inhibitor isolated from the marine sponge *Neopetrosia exigua*. *J. Am. Chem. Soc.* **2006**, *128*, 16046–16047.
- (12) Kumar, S.; Malachowski, W. P.; DuHadaway, J. B.; LaLonde, J. M.; Carroll, P. J.; Jaller, D.; Metz, R.; Prendergast, G. C.; Muller, A. J. Indoleamine 2,3-dioxygenase is the anticancer target for a novel series of potent naphthoquinone-based inhibitors. *J. Med. Chem.* **2008**, *51*, 1706–1718.
- (13) Li, X.; Yin, W.; Sarma, P. V. V. S.; Zhou, H.; Ma, J.; Cook, J. M. Synthesis of optically active ring-A substituted tryptophans as IDO inhibitors. *Tetrahedron Lett.* **2004**, *45*, 8569–8573.
- (14) Gaspari, P.; Banerjee, T.; Malachowski, W. P.; Muller, A. J.; Prendergast, G. C.; DuHadaway, J.; Bennett, S.; Donovan, A. M. Structure–activity study of brassinin derivatives as indoleamine 2,3-dioxygenase inhibitors. *J. Med. Chem.* **2006**, *49*, 684–692.
- (15) Muller, A. J.; DuHadaway, J. B.; Donover, P. S.; Sutanto-Ward, E.; Prendergast, G. C. Inhibition of indoleamine 2,3-dioxygenase, an immunoregulatory target of the cancer suppression gene Bin1, potentiates cancer chemotherapy. *Nat. Med. (N.Y., NY, U.S.)* **2004**, *11*, 312–319.
- (16) Muller, A. J.; Malachowski, W. P.; Prendergast, G. C. Indoleamine 2,3-dioxygenase in cancer: targeting pathological immune tolerance with small-molecule inhibitors. *Expert Opin. Ther. Targets* **2005**, *9*, 831–849.
- (17) Ichikawa, T.; Kato, T.; Takenishi, T. New synthesis of adenine and 4-aminoimidazole-5-carboxamide. *J. Heterocycl. Chem.* **1965**, *2*, 253–255.
- (18) Kocevar, M.; Polanc, S.; Sollner, M.; Tisler, M.; Vercek, B. Simple procedure for the synthesis of pyridinecarboximidoyl chlorides and bromides. *Synth. Commun.* **1988**, *18*, 1427–1432.
- (19) Andrianov, V.; Eremeev, A. 4-Aminofurazan-3-carboximidic acid halides. *Khim. Geterotsikl. Soedin.* **1994**, 420–425.
- (20) Gajewski, T. F.; Meng, Y.; Harlin, H. Immune suppression in the tumor microenvironment. *J. Immunother.* **2006**, *29*, 233–240.
- (21) Oda, S. I.; Sugimoto, H.; Yoshida, T.; Shiro, Y. Crystallization and preliminary crystallographic studies of human indoleamine 2,3-dioxygenase. *Acta Crystallogr., Sect. F: Struct. Biol. Cryst. Commun.* **2006**, *F62*, 221–223.
- (22) Buzykin, B. I.; Dokuchaev, A. S.; Kharitonova, O. A. Crystal and molecular structure of *N*-phenyl-4-nitrobenzamidoxime. *Izv. Akad. Nauk, Ser. Khim.* **1995**, 1516–1519.
- (23) Hou, D.-Y.; Muller, A. J.; Sharma, M. D.; DuHadaway, J.; Banerjee, T.; Johnson, M.; Mellor, A. L.; Prendergast, G. C.; Munn, D. H. Inhibition of indoleamine 2,3-dioxygenase in dendritic cells by stereoisomers of 1-methyl-tryptophan correlates with antitumor responses. *Cancer Res.* **2007**, *67*, 792–801.